Supplement of

Quantifying the impacts of human water use and climate variations on recent drying of Lake Urmia basin: the value of different sets of spaceborne and in-situ data for calibrating a hydrological model

Hosseini-Moghari et al.

Correspondence to: Seyed-Mohammad Hosseini-Moghari (Hosseini_sm@igsnrr.ac.cn)

1 WaterGAP

WaterGAP is a global hydrological model for assessing water resources under the influence of humans (Döll et al., 2003; Müller Schmied et al., 2014). With a spatial resolution of 0.5°×0.5°, it simulates water abstractions and consumptive water use (so-called net abstractions, i.e. the amount of water that evapotranspirates during use and does not flow to surface water bodies and groundwater afterwards) in five sectors (irrigation, livestock, domestic, manufacturing and cooling of thermal power plants, see Fig. S1); then net abstractions from either groundwater (NAg) or surface water bodies (NAs) are computed (Müller Schmied et al., 2014; Döll et al., 2012). Negative values of NAg occur where return flow to groundwater from irrigation with surface water is so high that water is added to groundwater storage by human water use. NA is the sum of NAg and NAs and equal to consumptive water use. Time series of NAg and NAs in each grid cells are then input to the WaterGAP Global Hydrology model WGHM that simulates their effect on water flows and storages (see Fig. S2). In WGHM, NAg and NAs are subtracted from either the groundwater or surface water bodies (lakes, reservoirs or rivers) (Müller Schmied et al., 2014).

WGHM simulates daily water storage as well as flows like evapotranspiration, groundwater recharge (Döll and Fiedler, 2008), runoff, and river discharge for all continents except Antarctica. Water is transported between grid cells according to the DDM30 drainage direction map (Döll et al., 2003). Water storage compartments encompass snow, canopy, soil, groundwater, rivers, lakes, wetlands, and man-made reservoirs (Eicker et al., 2014). Lake water storage is simulated as the difference of precipitation on the lake, evapotranspiration, inflows, and outflows. Outflow is zero for end lakes like Lake Urmia. The temporal variation of lake area, affecting precipitation on and evapotranspiration from the lake, is simulated as a non-linear function of lake water storage. WGHM contains more than 20 parameters that can be potentially be adjusted by calibration (Werth and Güntner, 2010).

WaterGAP includes a multitude of global data sets including information on irrigated areas, the fraction of irrigated areas that are equipped to be irrigated with groundwater (Siebert et al., 2010) and artificial drainage affecting return flows to surface water (Döll et al., 2012). For more information on data and model algorithms used in WaterGAP please refer to Müller Schmied et al. (2014) and Döll et al. (2014a). WaterGAP outputs were extensively compared to in-situ streamflow observations (e.g., Döll et al., 2003; Müller Schmied et al., 2014), to GRACE TWSA (Döll et al., 2012; Döll et al., 2014a) and GPS TWSA (Döll et al., 2014b). Results were shown to depend on applied climate input data sets (e.g., Müller Schmied et al., 2014, 2016; Döll et al., 2014b), model structure (Müller Schmied et al., 2014), and assumptions on water use (Döll et al. 2014a; Döll et al. 2014b). Comparison of observed streamflow regime indicators (different streamflow percentiles representing statistical low and high flows) to the values computed by nine (or seven) GHMs showed that WaterGAP is one of the best fitting models (Gudmundsson et al. 2012; Tallaksen and Stahl, 2014). Prudhomme et al. (2011) concluded that “of the three global models considered here, WaterGAP is arguably best suited to reproduce most regional characteristics of large-scale high and low flow events in Europe.” Regarding the fit to GRACE and GPS TWS, Döll et al. (2014b) found that WaterGAP underestimates seasonal variations of TWS on most of the land area of the globe and that seasonal maximum TWS occurs one month earlier according to WaterGAP than according to GRACE on most land areas.

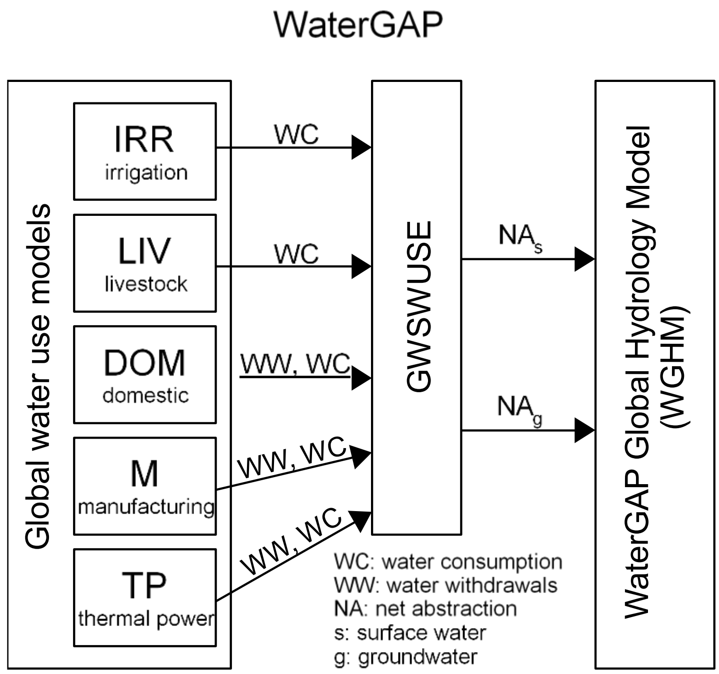

Figure S1: Schematic of WaterGAP. The outputs of Ground Water-Surface Water USE submodel (GWSWUSE) for five sectors are translated into NAg and NAs, respectively, which allows computing the impact of human water use on storages and water flows by WGHM. For details see Döll et al. (2012).

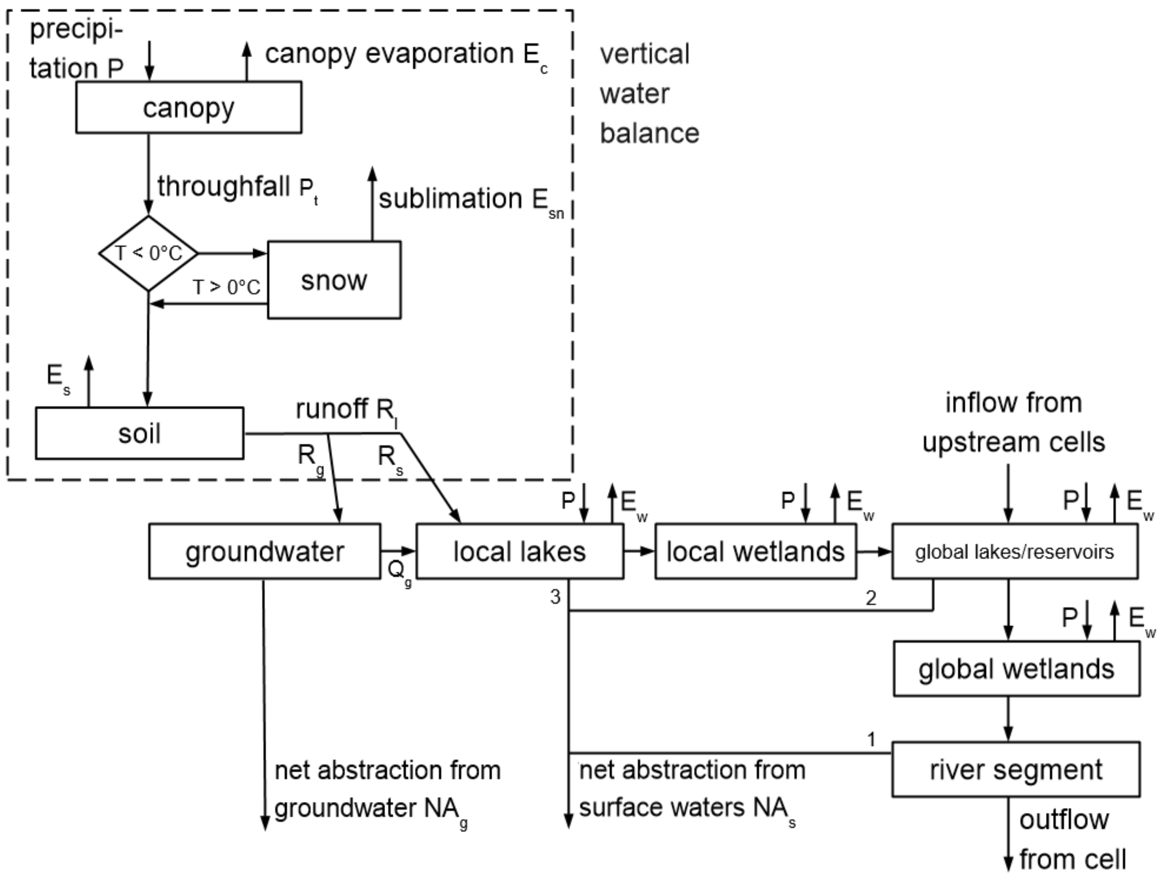

Figure S2: Schematic of WGHM within each 0.5◦ grid cell. Arrows represent water fluxes (inflows, outflows) and boxes show the water storage compartments. For details see Müller Schmied et al. (2014).

2 Data

2.1 Remote sensing data

Irrigated area in Lake Urmia basin. Based on MODIS images, Kamali and Youneszadeh Jalili (2015) estimated the annual time series of irrigated areas in Lake Urmia basin from 2001 to 2012. Considering that water management in the basin aims at preventing any increase of irrigated areas, it is assumed that the irrigated area in 2013 remained at the 2012 value (Fig. S3).

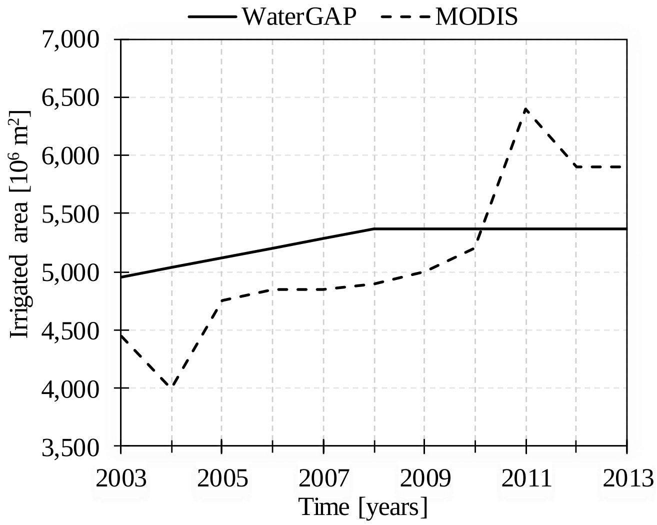

Figure S3: Irrigated area in Lake Urmia basin assumed in WaterGAP and derived from MODIS (data from Kamali and Youneszadeh Jalili, 2015).

GRACE total water storage anomalies. GRACE satellite data allow derivation of monthly time series of total water storage anomalies (TWSA) over all continents. TWSA describes the total amount of water stored on the continents, including water storage in surface water bodies, groundwater and soil, as compared to the mean value of total water storage over a reference period. In our study CSR GRACE RL05 mascon solutions (Save et al., 2016; http://www2.csr.utexas.edu/grace/RL05_mascons.html, last access: 17 July 2018) were used. While it is recommended GRACE data products only for areas with at least 100,000 km^2 (Watkins et al., 2015; Landerer and Swenson, 2012), studies by Tourian et al. (2015) and Lorenz et al. (2014) showed that signal strength or the so-called gravimetric resolution is determining the applicability of GRACE data. In fact, Lake Urmia basin has experienced an $8 \cdot 10^9$ m^3 change in the water volume in the last decade, which allows the use of GRACE for monitoring the changes in water storage in the basin (Tourian et al., 2015). This fact is supported by the very small gain factor of 1.0083 for the Lake Urmia basin based on Community Land Model 4 (CLM4) for spherical harmonic solutions (Landerer and Swenson, 2012), which is the factor with which signal attenuation due to leakage could be balanced. We can assume errors of the applied GRACE monthly time series of TWSA are small compared to the uncertainty of TWSA as computed by WGHM, such that model calibration against GRACE TWSA is meaningful.

2.2 Inflow into Lake Urmia

We used total annual observed inflow into the lake during 2003-2013 which was computed by the Urmia Lake Restoration Program (ULRP) based on 19 hydrometric stations around the lake (data available in http://ulrp.sharif.ir/ (In Persian), last access: 12 November 2017). Monthly observations were not available. It was compared to the sum of simulated river discharge of all WGHM grid cells flowing into the grid cell representing Lake Urmia.

2.3 Groundwater levels and groundwater storage

For evaluating the groundwater status in Lake Urmia basin, we used groundwater head data of 284 wells during 2003-2013 (Fig. 3). To obtain a monthly time series of average groundwater level in the basin, first the average of all groundwater level in each 0.5° grid cell was calculated and then the average values of all grid cells (see Strassberg et al., 2009). Using the results of a manual calibration for the RS_Q_GW_NA variant, which was the most comprehensive calibration variant, we estimated the average specific yield of the aquifers in the Lake Urmia Basin, i.e. the change in groundwater storage per unit change of the elevation of the groundwater table. We first divided the standard deviation of the simulated groundwater storage time series by the basin area to obtain groundwater storage variability in terms of equivalent water height and then divided this value by the standard deviation of the observed groundwater levels. This resulted in a specific yield estimate of 0.02, which is equal to the average value derived from pumping tests at 10 locations south of the lake (Hamzekhani and Aghaie, 2015). Using specific yield and observed groundwater level, we estimated the groundwater storage anomaly (GWSA) over the basin.

2.4 Water withdrawals and consumptive uses

There are no water withdrawals time series data in Lake Urmia basin. However, water withdrawals in the Lake Urmia basin for 2009 were reported to be $4{,}825 \cdot 10^6$ m^3 (ULRP, 2015) of which 89% is used for irrigation (Table S1). 57% of the withdrawn water is taken from surface water, the rest from groundwater. According to the report of Mahab Ghodss Consulting Engineering (2013), 16% of the water withdrawn for irrigation returns to groundwater and only 2% to surface water bodies, while the respective values for industrial and domestic water withdrawals are 50% and 10%. In our study, observed consumptive irrigation use was computed by subtracting total return flow from total water withdrawals for irrigation. Thus, consumptive use for irrigation was assumed to be 82% of water withdrawals for irrigation and 40% of the domestic and industry water withdrawals. The sum of consumptive water use in all sectors is the so-called total net abstraction (NA) from either surface water bodies or groundwater.

Table S1: Water withdrawals in Lake Urmia basin in 2009 [10^6 m^3] (data from URLP, 2015).

Source	Sector			Total
	Agricultural	Domestic	Industry	
Surface water	2424	276	33	2733
Groundwater	1867	190	35	2092
Total	4291	466	68	4825

2.5 Climate

The 0.5° gridded EartH2Observe, WFDEI and ERA-Interim Data Merged and Bias-corrected for ISIMIP (EWEMBI) dataset (Lange, 2016) were used as forcing data set. EWEMBI includes daily climate data from 1979 to 2013. For EWEMBI, ERA-Interim Reanalysis Data were bias-corrected with monthly observation data on temperature, precipitation and the number of wet days as well as daily radiation data. We compared, for the period 2003-2013, basin-average monthly precipitation and temperature values of EWEMBI dataset with those derived as the mean over monthly values observed at 143 rain gauges and six temperature gauging stations. The correlation coefficient (CC), Nash-Sutcliffe efficiency (NSE), and Willmott's refined index of agreement (Willmott et al., 2012) were 0.985, 0.946, and 0.897, respectively, for precipitation, and 0.996, 0.983, and 0.941 respectively, for temperature.

2.6 Lake volume

Based on remote sensing data for lake extent and water table elevation as well as on in-situ bathymetry data, a time series of monthly water volume in Lake Urmia for the period 2003-2013 was generated by Tourian et al. (2015) (their Fig. 9). It was used for evaluation of the calibrated model.

3 Calibration variants

3.1 RS variant: Calibration using remote sensing data

Irrigated area in Lake Urmia basin used in the standard version of WaterGAP is larger than the MODIS-based irrigated area until 2010, and smaller afterward (Fig. S3). The largest differences, in 2004 and 2011, exceed 20%, or 1,000 km^2, and the strongly increasing trend is not represented in WaterGAP. The constant value of the irrigated area in WaterGAP is due to the fact that the Food and Agricultural Organization of the UN does not provide more recent estimates of irrigated area in Iran (see http://www.fao.org/nr/water/aquastat, last access: 13 February 2018). To utilize the MODIS-based time series, consumptive irrigation water use in the whole basin of WaterGAP in year i was first adjusted by multiplying it by a correction factor CF1(i), with:

$$CF1(i) = \frac{Area_{irri}^{MODIS}(i)}{Area_{irri}^{WG}(i)} \quad \text{(S1)}$$

where $Area_{irri}^{MODIS}(i)$ is irrigated area from MODIS in year *i* and $Area_{irri}^{WG}(i)$ is irrigated area from WaterGAP database. The modified consumptive irrigation use was then added to the consumptive use of WaterGAP for the other sectors to obtain an updated basin-wide NA for each year. Then, modified monthly NAg and NAs in year *i* were calculated by multiplying, for each grid cell, the standard WaterGAP NAg and NAs values with the ratio of modified over standard basin-wide NA in year *i*. Then, WGHM was run using GA algorithm until achieving a good fit to monthly time series of basin-average GRACE TWSA (Fig. 4, mustard lines).

3.2 RS_Q_GW_NA variant: Calibration using remote sensing data, inflow into the lake, groundwater level, and net abstractions

In this calibration variant, statistical data on water withdrawals in 2009 (Table S1) was used together with information on return flow to compute a consumptive irrigation water use Cu_{irri}^{Obs} in the basin of 3,520·10^6 m^3. To estimate irrigation use in all other years, with different climatic conditions, the per area consumptive irrigation water use from WaterGAP was used to compute, for each year, a climatic correction factor CF2(i) as

$$CF2(i) = \left(\frac{Cu_{irri}^{WG}(i)}{Area_{irri}^{WG}(i)} - \frac{Cu_{irri}^{WG}(2009)}{Area_{irri}^{WG}(2009)}\right) \qquad \text{(S2)}$$

where $CF2(i)$ is represents the difference in the per area consumptive irrigation use in year *i* and the year 2009, $Cu_{irri}^{WG}(i)$ is consumptive irrigation use in year *i* obtained in standard WaterGAP. Finally, Eq. S3 was used for estimating water consumption time series over Urmia basin:

$$Cu_{irri}(i) = \left(\frac{Area_{irri}^{MODIS}(i)}{Area_{irri}^{MODIS}(2009)}\right) \times Cu_{irri}^{Obs}(2009) + CF2(i) \times Area_{irri}^{MODIS}(i) \qquad \text{(S3)}$$

where $Cu_{irri}(i)$ is consumptive irrigation water use in year *i*. Consumptive use of the other sectors was added based on withdrawal data in Table S1 and a return flow fraction of 60%, resulting in total NA. Keeping total NA(i) constant, correction factors $\alpha(i)$ and $\beta(i)$ were determined , with:

$$NA(i) = \alpha(i) \times NAs(i) + \beta(i) \times NAg(i) \qquad \text{(S4)}$$

Then, values for correction factors $\alpha(i)$ and $\beta(i)$ (Eq. S4) were identified by trial-and-error, and model parameters were modified to obtain a good fit to the data also used in the RS_Q_GW_NA variant.

4 Results of modifying NAs and NAg

In variant RS, annual time series of irrigated area in Lake Urmia basin derived from MODIS (Fig. S3), which were applied in both calibration variants, lead to a more strongly increasing trend of NA (consumptive water use) and NAs, as compared to the standard WaterGAP version (Fig. S4). Due to the dominant irrigation with surface water assumed in the standard version of WaterGAP, return flows from irrigation are larger than groundwater withdrawals, and there is a net recharge of groundwater by irrigation, i.e. a negative NAg. Therefore, a more strongly increasing irrigation with surface water in variant RS leads to return flows to groundwater that increase more strongly over time, i.e. NAg becomes increasingly negative with time (Fig. S4). Average NA in 2003-2010 decreased from 4,185·10^6 m^3/yr in the standard version to 3,815·10^6 m^3/yr, and increased from 4,233·10^6 m^3/yr to 4,781·10^6 m^3/yr in 2011-2013. However, increased net recharge of groundwater by return flows was found to be incompatible with decreasing observed groundwater storage (Fig. 7c). Positive NAg values were found to be necessary to simulate the observed lowering of groundwater storage from 2003 to 2013.

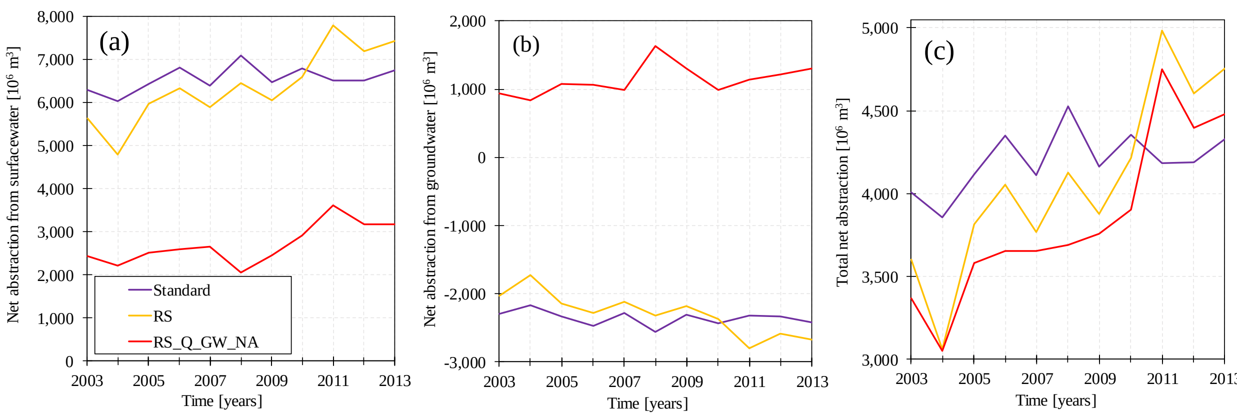

Figure S4: Time series of net abstractions from surface water (a) and groundwater (b), as well as total net abstractions (i.e. consumptive use) (c) in Lake Urmia basin in the standard version of WaterGAP as well as both calibration variants.

5. Supplement tables and figure

Table S2: Correction factors for modifying NAs and NAg (see Eq. S4).

Year	α	β
2003	0.39	-0.41
2004	0.37	-0.39
2005	0.39	-0.46
2006	0.38	-0.43
2007	0.42	-0.43
2008	0.29	-0.63
2009	0.38	-0.57
2010	0.43	-0.41
2011	0.56	-0.49
2012	0.49	-0.52
2013	0.47	-0.54

Table S3: Parametrization of GA and NSGA-II used in two calibration variants.

Parameter	GA	NSGA-II
Population	50	80
Generation	100	150
Selection function	Roulette wheel	Tournament
Crossover fraction	Two-point crossover	Two-point crossover
Crossover function	0.65	0.70
Mutation rate	Uniform	Uniform
Mutation function	0.05	0.05

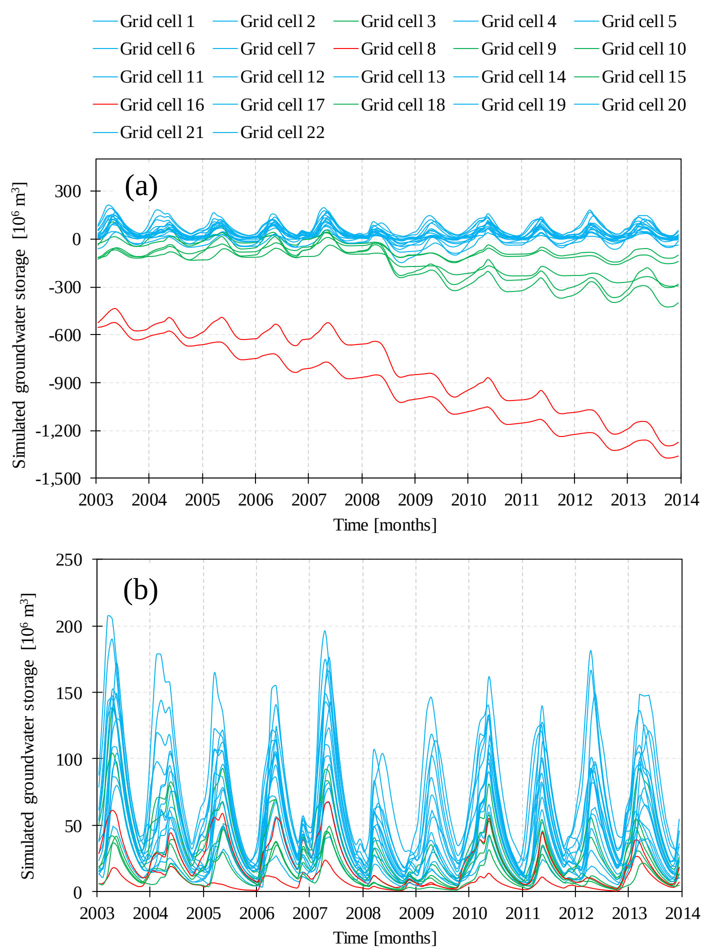

Figure S5: Simulated groundwater storage in each of the 22 0.5° grid cells in Lake Urmia basin under anthropogenically altered (Fig. S5a) and naturalized conditions (Fig. S5b).

References

Döll, P., and Fiedler, K.: Global-scale modeling of groundwater recharge, Hydrology and Earth System Sciences Discussions, 12, 863-885, doi:10.5194/hess-12-863-2008, 2008.

Döll, P., Fritsche, M., Eicker, A., Müller Schmied, H.: Seasonal water storage variations as impacted by water abstractions: Comparing the output of a global hydrological model with GRACE and GPS observations, Surveys in Geophysics, 35(6), 1311-1331, doi:10.1007/s10712-014-9282-2, 2014b.

Döll, P., Hoffmann-Dobrev, H., Portmann, F. T., Siebert, S., Eicker, A., Rodell, M., Strassberg, G., and Scanlon, B. R.: Impact of water withdrawals from groundwater and surface water on continental water storage variations, J. Geodyn., 59–60, 143–156, doi:10.1016/j.jog.2011.05.001, 2012.

Döll, P., Kaspar, F., and Lehner, B.: A global hydrological model for deriving water availability indicators: model tuning and validation, Journal of Hydrology, 270, 105-134, doi:10.1016/S0022-1694(02)00283-4, 2003.

Döll, P., Müller Schmied, H., Schuh, C., Portmann, F. T., and Eicker, A.: Global-scale assessment of groundwater depletion and related groundwater abstractions: Combining hydrological modeling with information from well observations and GRACE satellites, Water Resources Research, 50, 5698-5720, doi:10.1002/2014WR015595, 2014a.

Eicker, A., Schumacher, M., Kusche, J., Döll, P., and Schmied, H. M.: Calibration/data assimilation approach for integrating GRACE data into the WaterGAP Global Hydrology Model (WGHM) using an ensemble Kalman filter: first results, Surveys in Geophysics, 35, 1285-1309, doi:10.1007/s10712-014-9309-8, 2014.

Gudmundsson, L., Tallaksen, L. M., Stahl, K., Clark, D. B., Dumont, E., Hagemann, S., Bertrand, N., Gerten, D., Heinke, J., Hanasaki, N., Voss, F., and Koirala, S.: Comparing Large-Scale Hydrological Model Simulations to Observed Runoff Percentiles in Europe, Journal of Hydrometeorology, 13, 604-620., doi:10.1175/JHM-D-11-083.1, 2012.

Hamzekhani, H., and Aghaie, M. M.: Miandoab plain Groundwater modelling with the use of remote sensing technology to assess the impact of changes in aquifer conditions on surface flow, Report of Urmia Lake Restoration Program (ULRP) (In Persian), 2015.

Kamali, M., and Youneszadeh Jalili, S.: Investigation of landuse changes in Lake Urmia Basin using remotely sensed images, Report of Urmia Lake Restoration Program (ULRP) (In Persian), 2015.

Landerer, F. W., and Swenson, S. C.: Accuracy of scaled GRACE terrestrial water storage estimates, Water resources research, 48, doi:10.1029/2011WR011453, 2012.

Lange, S.: EartH2Observe, WFDEI and ERA-Interim data Merged and Bias-corrected for ISIMIP (EWEMBI), GFZ Data Services, doi:10.5880/pik.2016.004, 2016.

Lorenz, C., Kunstmann, H., Devaraju, B., Tourian, M. J., Sneeuw, N., and Riegger, J.: Large-scale runoff from landmasses: a global assessment of the closure of the hydrological and atmospheric water balances, Journal of Hydrometeorology, 15, 2111-2139, doi:10.1175/JHM-D-13-0157.1, 2014.

Mahab Ghodss consulting engineering: Report on the balance of water resources and consumption (40-year-average) in Lake Urmia Basin, Ministry of energy (In Persian), 2013.

Müller Schmied, H., Eisner, S., Franz, D., Wattenbach, M., Portmann, F. T., Flörke, M., and Döll, P.: Sensitivity of simulated global-scale freshwater fluxes and storages to input data, hydrological model structure, human water use and calibration, Hydrology and Earth System Sciences, 18, 3511-3538, doi:10.5194/hess-18-3511-2014, 2014.

Prudhomme, C., Parry, S., Hannaford, J., Clark, D. B., Hagemann, S., and Voss, F.: How Well Do Large-Scale Models Reproduce Regional Hydrological Extremes in Europe?, Journal of Hydrometeorology, 12, 1181-1204, doi:10.1175/2011JHM1387.1, 2011.

Save, H., Bettadpur, S., and Tapley, B. D.: High-resolution CSR GRACE RL05 mascons, Journal of Geophysical Research: Solid Earth, 121, 7547-7569, doi:10.1002/2016JB013007, 2016.

Siebert, S., Burke, J., Faures, J.-M., Frenken, K., Hoogeveen, J., Döll, P., and Portmann, F. T.: Groundwater use for irrigation–a global inventory, Hydrology and Earth System Sciences, 14, 1863-1880, doi:10.5194/hess-14-1863-2010, 2010.

Strassberg, G., Scanlon, B. R., and Chambers, D.: Evaluation of groundwater storage monitoring with the GRACE satellite: Case study of the High Plains aquifer, central United States, Water Resources Research, 45, doi: 10.1029/2008WR006892, 2009.

Tallaksen, L. M. and Stahl, K.: Spatial and temporal patterns of large-scale droughts in Europe. Model dispersion and performance, Geophysical Research Letters, 41, 429-434, doi:10.1002/2013GL058573, 2014.

Tourian, M. J., Elmi, O., Chen, Q., Devaraju, B., Roohi, S., and Sneeuw, N.: A spaceborne multisensor approach to monitor the desiccation of Lake Urmia in Iran, Remote Sensing of Environment, 156, 349-360, doi:10.1016/j.rse.2014.10.006, 2015.

ULRP: Status of water resources and water consumption in the basin, Available at: http://ulrp.sharif.ir/fa (In Persian), last access: 17 July 2018, 2015.

Watkins, M. M., Wiese, D. N., Yuan, D. N., Boening, C., and Landerer, F. W.: Improved methods for observing Earth's time variable mass distribution with GRACE using spherical cap mascons, Journal of Geophysical Research: Solid Earth, 120, 2648-2671, doi:10.1002/2014JB011547, 2015.

Werth, S., and Güntner, A.: Calibration analysis for water storage variability of the global hydrological model WGHM, Hydrology and Earth System Sciences, 14, 59, doi:10.5194/hess-14-59-2010, 2010.

Willmott, C. J., Robeson, S. M., and Matsuura, K.: A refined index of model performance, International Journal of Climatology, 32(13), 2088-2094, doi:10.1002/joc.2419, 2012.